COMPUTER METHODS AND PROGRAMS IN BIOMEDICINE 107 (2012) 28–35

journal homepage: www.intl.elsevierhealth.com/journals/cmpb

In quest of the missing neuron: Spike sorting based on dominant-sets clustering

Dimitrios A. Adamos[a,*], *Nikolaos A. Laskaris*[b], *Efstratios K. Kosmidis*[c], *George Theophilidis*[a]

[a] *Laboratory of Animal Physiology, School of Biology, Aristotle University of Thessaloniki, 54 124 Thessaloniki, Greece*
[b] *Laboratory of Artificial Intelligence and Information Analysis, Department of Informatics, Aristotle University of Thessaloniki, 54 124 Thessaloniki, Greece*
[c] *Laboratory of Physiology, School of Medicine, Aristotle University of Thessaloniki, 54 124 Thessaloniki, Greece*

ARTICLE INFO

Article history:
Received 20 February 2011
Received in revised form
28 October 2011
Accepted 30 October 2011

Keywords:
Sparsely-firing neuron
Graph-theoretic clustering
ISOMAP
Dominant sets

ABSTRACT

Spike sorting algorithms aim at decomposing complex extracellular signals to independent events from single neurons in the electrode's vicinity. The decision about the actual number of active neurons is still an open issue, with sparsely firing neurons and background activity the most influencing factors. We introduce a graph-theoretical algorithmic procedure that successfully resolves this issue. Dimensionality reduction coupled with a modern, efficient and progressively executable clustering routine proved to achieve higher performance standards than popular spike sorting methods. Our method is validated extensively using simulated data for different levels of SNR.

1. Introduction

The basis of every spike sorting algorithm is the assumption that all the action potential traces of a particular neuron have nearly the same amplitude and shape. In extracellular recordings, the shapes of neural waveforms reflect the neuron's geometry and its distance to the recording electrode [1,2]. The goal of a spike sorting process is to identify the number of active neurons and extract detailed time courses of their spiking activity from extracellular neural recordings. The related algorithms display a variety of applications ranging from clinical neurophysiology to cortex–machine interfaces.

The battery of available spike sorting routines includes mainly automated techniques that analyze the recorded signals by means of their waveforms. In a first step, linear techniques like principal component analysis (PCA) [3,4] and wavelets [5–7] are often employed to reduce the dimensionality of the input data and enhance the signal dynamics. PCA representation is most often restrained within the subspace spanned by the first two or three principal components, although the incorporation of additional components is often advantageous [8]. Alternatively, the wavelet transform can be employed in the representation step so as to enhance the subsequent spike discrimination by emphasizing particular morphological characteristics. In both cases, the representation step serves as a preprocessing stage for a clustering framework that would take over the detection of distinct signal sources (i.e. active neurons) and the classification of the corresponding spiking contributions.

* Corresponding author. Tel.: +30 2310 998261/991839; fax: +30 2310998269.
E-mail addresses: dadam@bio.auth.gr, d.adamos@ieee.org (D.A. Adamos), laskaris@aiia.csd.auth.gr (N.A. Laskaris), kosmidef@med.auth.gr (E.K. Kosmidis), theophil@bio.auth.gr (G. Theophilidis).
0169-2607/$ – see front matter © 2011 Elsevier Ireland Ltd. All rights reserved.
doi:10.1016/j.cmpb.2011.10.015

Regarding clustering, Bayesian [9] and expectation maximization [10] methods have been proposed for spike sorting. A stationary Gaussian profile for the background noise is a popular assumption in the related methodologies [11]. Both the above methods consider Gaussian characteristics for the potential clusters residing in the PCA representation subspace. However, background noise in realistic neural recordings may only be approximately modeled as stationary Gaussian process [12]. Actually, deviations from stationarity and normality are the usual case. Synaptic coupling among neurons, superimposed field potentials, electrode drifts and bursting neurons are all factors that constitute a non-stationary non-Gaussian cluster profile more plausible [7,9,13–15]. To avoid Gaussian considerations, clustering approaches featuring hierarchical algorithms have appeared [7,16]. In particular, the work described in [7], namely *Waveclus*, is currently considered as a state-of-the-art technique in the spike sorting domain [17]. It employs a stochastic algorithm, known as super-paramagnetic clustering (SPC), which makes no prior assumptions about the statistical properties of the data. Furthermore, online spike sorting techniques have appeared incorporating data-dependent feedback so as to directly adapt to the non-stationarities of the recording [18].

There are two important parameters when one evaluates a spike sorting classification process: the number of clusters (i.e. the number of active neurons) being decided by the process and the number of spikes assigned to each cluster. Both are well incorporated by Type I/II errors [10] in the spike sorting domain. Type I (false positive (FP))/II (false negative (FN)) errors derive from the traditional classification schemes and conceptualize misclassification. A false-positive corresponds to a misplaced spike (most often represented by an ambiguous waveform), wrongly assigned to the cluster of waveforms for a particular neuron. Likewise, a false-negative corresponds to a spike missing from the cluster of a neuron's waveforms. Thus, the identification of fewer neurons than expected (under-clustering) leads to high false positive errors, while the opposite case (over-clustering) results in a large amount of false negatives. Although a correct estimation of the number of clusters would limit both errors in cluster-delineation, the identification of the actual number of active neurons is still an open issue. Even popular methods (like SPC) do not often incorporate a satisfactory treatment of this issue, leading to erroneous results [17]. It is worth noting that, in laboratory practice, over-clustering is most often addressed in a less time-consuming way than under-clustering. In a recently published work [8], we have stressed the importance of the previous fact and defined a new clustering-error measure that penalizes under-clustering more than over-clustering.

There are two main reasons that obstruct the estimation of the 'true' number of active neurons. The first relates to the low SNR of the signals and the subsequent poor representation (in the original or reduced space) of the waveforms. The second relates to the existence of sparsely firing neurons among those contributing to the recorded signal. The identification of the relatively rare events corresponding to their activations is an issue left untreated by the vast majority of contemporary algorithms targeting the activity of dominating 'hyperactive' neurons. However, the involvement of this type of neurons in the formation of neural code has been recently emphasized [19–23] and the development of a spike sorting algorithm capable of recognizing sparsely-firing neurons is necessary. Currently, only Waveclus has been considered as 'an optimal spike sorting algorithm that is particularly suited to detect sparsely firing neurons, which typically have very low baseline firing rates' [21].

Here we propose a sequential, subtractive algorithmic procedure which, apart from the reliable classification of activations from 'conventional' neurons, can treat equally well activations from 'occasional' or 'sporadic' neurons. The principal algorithm stems from graph theoretic ideas and in particular the notion of dominant sets [24]. It works in an iterative fashion by operating on a neighborhood graph. It identifies the core of the graph, using replicator dynamics formulation, and then removes it from the graph and feeds back the remaining graph. The procedure terminates when all the data have been assigned to distinct groups or no more compact groups can be formed. The incorporated algorithm is engaged to work within a representation space which is derived via a fully compatible dimensionality reduction technique, namely the isometric feature mapping (ISOMAP) [25]. ISOMAP is known to reveal the intrinsic data variation and is therefore expected to be insensitive to random variations due to background noise. Hence, the resulting low-dimensional parameterization of the waveform variation is expected to enhance the clustering performance.

A preliminary version of this work has appeared in the Proceedings of the 12th Mediterranean Conference on Medical and Biological Engineering and Computing (MEDICON2010) [26]. The use of iterative dominant-sets algorithm for spike sorting was originally introduced therein. Here the algorithm is incorporated in a noise-assisted, pattern-analytic framework and extensively evaluated (A Matlab implementation of the algorithm is available online at http://neurobot.bio.auth.gr/spike-sorting).

The remainder of this article is organized as follows. Section 2 describes the proposed methodology. Section 3 presents the comparative evaluation of our spike sorting technique in relation with a state-of-the-art alternative [7], using simulated data. Section 4 concludes the paper.

2. Method

2.1. Low-dimensional representation

The neural waveform segments, extracted from the time-series of extracellular recordings, are considered as the initial raw representation of spiking activity. The ensemble of these loosely aligned spike-waveforms can be thought as a point-swarm residing in a multidimensional feature space with axes corresponding to signal amplitudes at particular latencies. Following the standard convention, the ith spike waveform is depicted as $x_i(t)$, $t = 1, 2, \ldots, T$, $i = 1, 2, \ldots, N$ (with t denoting discrete time or latency) and represented via the row-vector $\mathbf{x_i} = [x_i(1), x_i(2), \ldots, x_i(t), \ldots, x_i(T)] \in R^T$. Similarly the whole ensemble is represented in a data-matrix format as $\mathbf{X_{[N\times T]}} = [\mathbf{x_1}|\ \mathbf{x_2}|\ldots\ \mathbf{x_i}\ |\ldots\ \mathbf{x_N}]$, where '|' denotes a line separator.

Here, we employ ISOMAP embedding as a dimensionality reduction (denoising) step. The goal is to achieve a

parsimonious representation, in which the true degrees of freedom can be recognized and directly associated with involved neurons. The algorithmic details of ISOMAP technique can be found elsewhere [27,28]. It starts by building a neighborhood graph over the data-points in the original feature space. This graph is then used to compute all the geodesic inter-point distances. Multidimensional scaling is finally employed to derive a reduced coordinate space where these distances are preserved and therefore the intrinsic geometry of the data is faithfully represented. In our case, the ISOMAP-routine provides a geometrical picture, within an r-D space, of the spike-waveforms variation.

$$\mathbf{Y}_{[\mathbf{N}\times\mathbf{r}]} = [\mathbf{y_1}|\,\mathbf{y_2}|\ldots\mathbf{y_i}|\ldots\,\mathbf{y_N}] = \mathrm{ISOMAP}(\mathbf{X}, r) \tag{1}$$

where $\mathbf{y_i} = [y_i(1), y_i(2), \ldots, y_i(r)] \in R^r$.

The decision on the optimum (r_0) dimensionality of the r-D ISOMAP representation of the derived point-swarm (for a 2D example, see Fig. 1b) depends on the *residual variance* (the residual variance metric is a performance index ranging from 0% to 100%, indicating the reliability of the mapping). Details on the selection of optimum r_0 value can be found elsewhere (e.g. [28]).

2.2. *Detecting compact groups via dominant-sets approach*

A recently introduced graph-theoretic algorithm [24] is employed for identifying the most-cohesive groups of vertices, given the weighted similarity (adjacency) matrix of a graph. The algorithm is based on the identification of the dominant set of nodes and when repeatedly applied facilitates the effective clustering, in a sequential mode, of pairwise relational data. As stated in [24], 'the main property of a dominant set is that the overall similarity among internal nodes is higher than that between external and internal nodes, and this fact is the motivation of considering a dominant set as a cluster of nodes'.

One of its main characteristics is the compact, elegant formulation. In our case, the ISOMAP-representation points ($\mathbf{Y}$) are used to build an undirected edge-weighted, fully connected graph with no self-loops $G = (V, E, w)$, where $V = \{1, \ldots, N\}$ is the vertex set, $E \subseteq V \times V$ is the edge set and w: $E \to R_+^*$ is a positive weight function. The vertices correspond to data points and the edge-weights reflect similarity between pairs of vertices.

In a preprocessing step, the Euclidean inter-point distances $d_{ij} = ||\mathbf{y_i} - \mathbf{y_j}||_{L2}$ are transformed to similarity weights, based on a monotonic transformation:

$$w(i, j) = \exp\left(\frac{-d_{ij}}{\sigma}\right) \tag{2}$$

where σ is a real positive number reflecting the 'radius of influence' within the ISOMAP representation space. It is a crucial parameter, as it controls the clustering resolution. A high value would finally lead to under-clustering, while a low value to over-clustering. The optimal value of σ is defined in a data-dependent manner, during a separate stage, described later in the subsection devoted to the algorithmic implementation of our approach.

With the above notation, the N-node graph $G(V, E, w)$ built over the available data points can be represented with the similarity matrix $\mathbf{A}_{[\mathbf{N}\times\mathbf{r}]}$, with elements $A_{ij} = w(i, j)$ and $A_{ii} = 0$. The cohesiveness of a given group of points is measured by the overall similarity, which is estimated based on the corresponding entries in $\mathbf{A}$. A good cluster-candidate consists of elements that have large values connecting one another in the similarity matrix. Hence, the problem of finding a compact cluster is formulated as the problem of finding a vector $\mathbf{m}$ that maximizes the following objective function [24]:

$$\mathbf{F}(\mathbf{m}) = \mathbf{m}^T\mathbf{A}\mathbf{m} \tag{3}$$

subject to $\mathbf{m} \in \Delta$, where $\mathbf{\Delta} = \{\, m \in R^N : m_i \geq 0 \quad \forall i \quad \wedge \sum_{i=1}^{N} m_i = 1\}$.

The algorithmic procedure described in [24], detects the maximally cohesive cluster. Its operation is denoted as:

$$\{\mathbf{m}, \mathrm{F}(\mathbf{m})\} = \mathrm{Dominant\_Set}(\mathbf{A}) \tag{4}$$

The vector $\mathbf{m}$ lists the memberships for all nodes in the graph and can be used to identify the exact list of nodes participating in the dominant-set (by locating the non-zero elements). The second output $F(\mathbf{m})$ is the particular value of objective function that measures the cohesiveness of the detected dominant-set. The overall clustering procedure, proceeds in iterative fashion. The nodes participating in the dominant-set (at the end of a single execution of the Dominant_Set-routine) are removed from the graph and the associated entries in matrix $\mathbf{A}$ are zeroed. Then, the next dominant-set is delineated by working with the residual graph. The procedure terminates when the cohesiveness of the lastly formed group drops below a predefined threshold (here selected as the $F(\mathbf{m_0})$ value, with $\mathbf{m_0}$ the all-one vector, that corresponds to the cohesiveness-level when all the points are considered as members in a single group). The detected groups are ranked according to cohesiveness and a diagram summarizing the intermediate steps is produced (for an example, see Fig. 1d) and exploited for the exact definition of cluster numbers (i.e. the actual number of neurons).

The extensive experimentation with the dominant-sets algorithm, based on realistically simulated data, showed that the above described procedure was sufficient for grouping together spike-waveforms originating from the same neuron, even in cases of very low firing-rate. However, a tendency for 'benign' over-clustering also became evident. The additionally formed groups consisted of overlapping waveforms (an 'overlap' is a spike-waveform corresponding to co-firing, i.e. simultaneous activation, of a particular pair of active neurons). Such composite waveforms have to undergo a separate decomposition step (e.g. [28–30]) before used to assign spike-counts to the contributing neurons. For the purpose of this work, it was sufficient to develop a technique that could differentiate between a group of spike-waveforms from a particular single neuron (even if it was a sparsely firing one) and a group of overlapping spike-waveforms (that should be treated differently). The adopted solution was based on the conjecture that the cohesiveness of any group of waveforms from

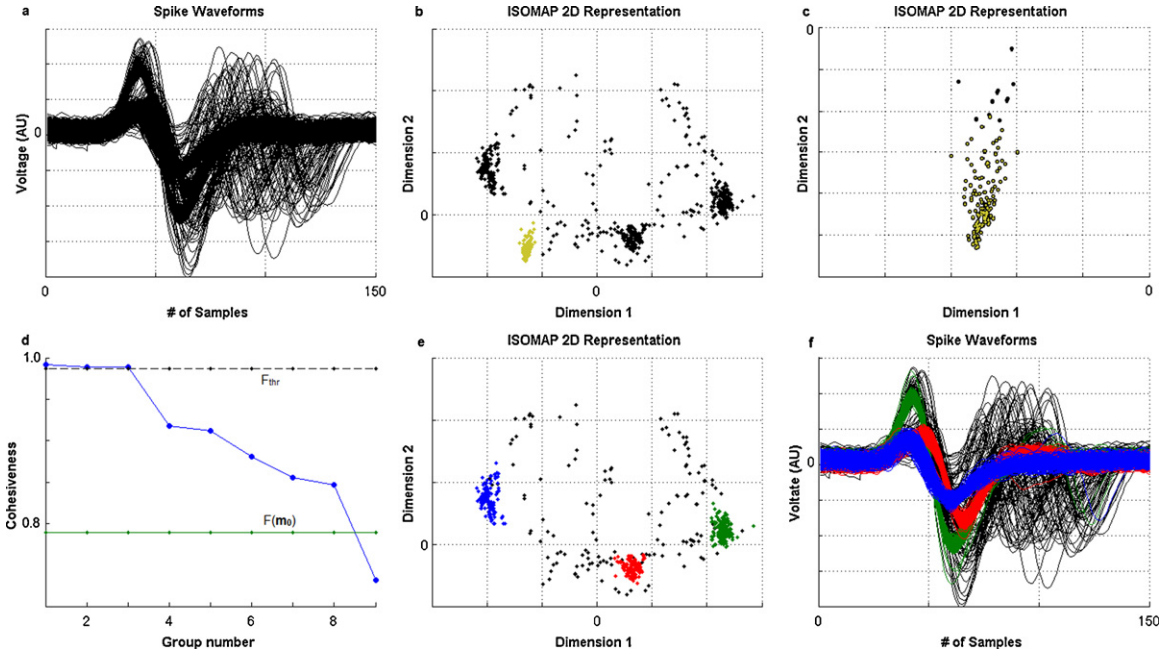

Fig. 1 – (a) The overall spike waveforms set (the SNR of this particular dataset is 4). (b) 2D ISOMAP representation of the data set. (c) The dominant-set extracted from the images of noise segments, corresponding to the optimal value σ_{sel}. (d) The cohesiveness values for the progressively formed groups. (e) Classification results visualized within 2D ISOMAP space. Colors indicate classes. (f) Classification results presented in the original data domain using the corresponding colors.

a single neuron depends only on the fixed level of common background noise and that a group of overlapping waveforms (due to variable time-delay between the individual waveforms) would show lower cohesiveness. The idea was to estimate a 'baseline'-value for the cohesiveness F_{thr}, based on spike-free extracts (i.e. background noise segments) from the extracellular recordings, and apply it in a thresholding scheme that would operate in the ranked list of groups formed with the Dominant-Set procedure. Groups of lower than F_{thr} cohesiveness are directed to an overlap-resolving algorithm. The introduced strategy, in addition, enabled the choice of parameter σ in Eq. (2).

2.3. *Algorithmic implementation*

The suggested algorithmic procedure consists of the following three steps. The first one serves representation purposes. The second is a training step in which the involved parameters are tailored to the noise characteristics of the particular recording. The final step includes the execution of the Dominant-Set procedure with the optimal parameters and the classification of formed groups into "genuine" and "overlaps".

2.3.1. *Step_1: ISOMAP representation*

After applying a conventional spike-detector [7,9,31,32], spike waveforms are extracted and used, as described in Section 2.1, to fill the data-matrix $\mathbf{X}$. This matrix is augmented by time-series segments of equal length, extracted from latencies where the spike-detector was silent (and hence they were corresponding to background noise). By denoting with $\mathbf{x_i}$ and $\mathbf{z_j}$, respectively, the neural waveforms and the noise segments (and with N_x and N_z their corresponding populations), the mapping procedure can be written as: $\mathbf{Y}' = \text{ISOMAP}\ (\mathbf{X}', r_0)$ where $\mathbf{X}' = [\mathbf{x_1}|\ \mathbf{x_2}|\dots\ \mathbf{x_{Nx}}|\ \mathbf{z_1}|\ \mathbf{z_2}|\dots\ \mathbf{z_{Nz}}]$ and $\mathbf{Y}'_{[(Nx+Nz)\,x\,r]} = [\mathbf{y}'_1|\ \mathbf{y}'_2|\dots\ \mathbf{y}'_{Nx+Nz}] = [\mathbf{y}^x{}_1|\ \mathbf{y}^x{}_2|\dots\ \mathbf{y}^x{}_{Nx}|\ \mathbf{y}^z{}_{Nx+1}|\ \mathbf{y}^z{}_{Nx+2}|\dots\ \mathbf{y}^z{}_{Nx+Nz}]$.

2.3.2. *Step_2: defining 'radius of influence' (σ) and cohesiveness threshold (F_{thr})*

We first isolate the images of noise-segments $\mathbf{Y^Z}$ and use them to built a series of similarity matrices $\{\mathbf{A}(\sigma)\}$ by varying the parameter σ in Eq. (2). For each realization, we run iteratively the Dominant-Set procedure and finally we identify the optimal radius σ_{sel} as the smallest value for which the great majority (e.g. $0.95\,N_z$) of noise-segment images form a single compact graph-component that cannot be resolved further into groups. The cohesiveness corresponding to this dominant set is selected as the 'baseline' cohesiveness-level F_{thr}.

2.3.3. *Step_3: executing dominant-sets algorithm*

With the remaining coordinates of spike-waveforms $\mathbf{Y^X}$, and using the estimated radius σ_{sel}, we derive the 'tuned' similarity matrix $\mathbf{A}$. By iteratively applying the Dominant-Set procedure, we form groups of waveforms that are subsequently ranked according to cohesiveness. The groups with cohesiveness higher than F_{thr} are considered 'genuine' and used to estimate the spiking-activity of independent neurons. The rest groups are ambiguous overlaps and should be treated accordingly.

3. Validation results

3.1. Conventional scenario: no sparsely-firing neurons

For the evaluation of our method in the standard situation addressed by all spike-sorting algorithms, we utilized a simulated data set (data set #1 in [28]) that realistically represents neural activity from three separate neurons including randomly overlapping spikes. Three 'actual' action potential waveforms served as the initial templates. They had been recorded extracellularly from respiratory motoneurons of the beetle *Tenebrio molitor* [33], with a sampling frequency of 30 kHz and correspond to a time-window of 150 samples (i.e. a time duration of 5 ms). The selected templates were replicated multiple times and superimposed to segments of background noise extracted from the same recording. In order to pursue evaluation results under different SNR-levels, each extract of real background noise was modulated by a variable, positive amplitude factor φ. The SNR of the resulting waveform (template plus noise segment) was then defined as follows:

$$\mathrm{SNR} = \frac{\overline{\mathrm{RMS}}(\mathrm{data\_set})}{\phi \cdot \mathrm{RMS}(\mathrm{random\ noise\ extract})} \tag{5}$$

Three-hundred (300) waveforms per template were generated yielding 900 single spikes corresponding to the three neural classes in our data set. In addition, paired combinations among the three templates were realized by first inducing variable delays and then adding noise segments using amplitude factors so as to achieve a particular SNR-level. In this way 150 waveforms of double-overlaps were generated; 50 for each template pair. Finally, 50 more waveforms were added corresponding to overlaps from all three neurons, with their SNR-level adjusted accordingly. The whole procedure for building the data set was repeated 10 times, resulting into 10 versions which differed regarding the noise components added over the spike-waveforms. We first demonstrate our method and then proceed with a quantitative evaluation.

An instance of the complete dataset (1100 waveforms), corresponding to SNR = 4, is shown in Fig. 1a. The 2D ISOMAP representation of this dataset, augmented by 300 background noise-segments, is included in Fig. 1b, where the images of noise are shown as yellow dots. Considering the high density areas of the point swarm corresponding to spike-waveforms (1100 black dots), the existence of three clusters (hence, the presence of three active neurons) becomes apparent. The training step, in which the parameter σ has been tailored to the noise profile, is illustrated in Fig. 1c. The delineated dominant set (yellow circles) includes the majority of the noise segments (i.e. their images within ISOMAP space) into a single group. Using the estimated σ_{sel}, dominant-sets are extracted based on the ISOMAP-representation of spike waveforms shown in Fig. 1b. The cohesiveness-levels of the clusters subtracted by this iterative procedure are shown in Fig. 1d, where the baseline value F_{thr} is indicated via the black horizontal line. As it can be seen, only the three highest-rank groups are associated with cohesiveness exceeding the threshold value F_{thr}. In addition, the horizontal green line indicates the $F(\mathbf{m_0})$ value (i.e. the cohesiveness of the whole set of spike-waveforms taken as single group) which is the lower threshold below which the iterative process should be terminated. The waveforms corresponding to the three active neurons are classified accordingly, while the rest are left unclassified (overlaps or clutter). This data-sieving step is visualized in ISOMAP space (Fig. 1e) and in the original data domain (Fig. 1f) using a three-level color-code.

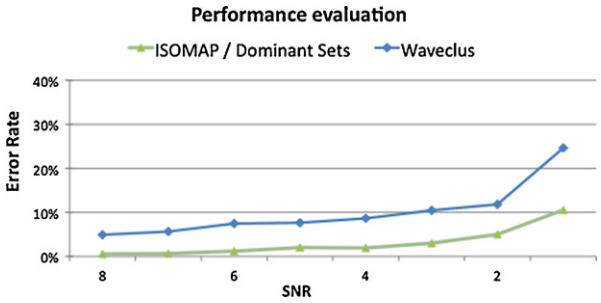

Fig. 2 – Average error rates for the proposed spike-sorting method and Waveclus.

Type I/II errors were used for the performance evaluation. The total number of FP and FN is referred to the identified classes (i.e. neurons). The adopted *error-rate* was defined as follows:

$$\text{Error-rate} = \frac{\Sigma_i(F_{P_i} + Fn_i)}{\text{Total \# of participating waveforms}} \times 100\% \tag{6}$$

with i running over the number of single-spike classes (i.e. the number of identified neurons). For comparison purposes, the measurements corresponding to Waveclus [7] are also included. Both Waveclus and our proposed methodology classified the spikes of the data set into three main classes. The overall results from the comparative study of these two spike-classification algorithms are shown in Fig. 2 (produced based on multiple realizations of the dataset and at different SNR-levels). The averaged (over realizations) error-rate is drawn as a function of SNR level. It can be seen that our approach achieves the lowest error rate which is not greater than 10% in all SNR cases.

3.2. Detecting a sparsely firing neuron

The proposed algorithm is further evaluated based on a scenario, in which a sparsely firing neuron is contributing to the recorded neural data. For simulating its contribution, we utilized an additional action potential template and augmented the previous data set (described in Section 3.1) by 30 related waveforms on which noise had been superimposed accordingly. As previously, 10 different realizations of this augmented dataset (by altering noise) were employed in validating the ability of our method to detect the sparsely-firing neuron at a particular SNR-level.

Fig. 3 visualizes the intermediate step and final result of our approach when applied to a particular dataset realization (corresponding to SNR = 4). As it can be seen in Fig. 3g, the waveforms of the 'sparse' neuron have all been grouped together (including two additional false-positive waveforms which will contribute to the error count).

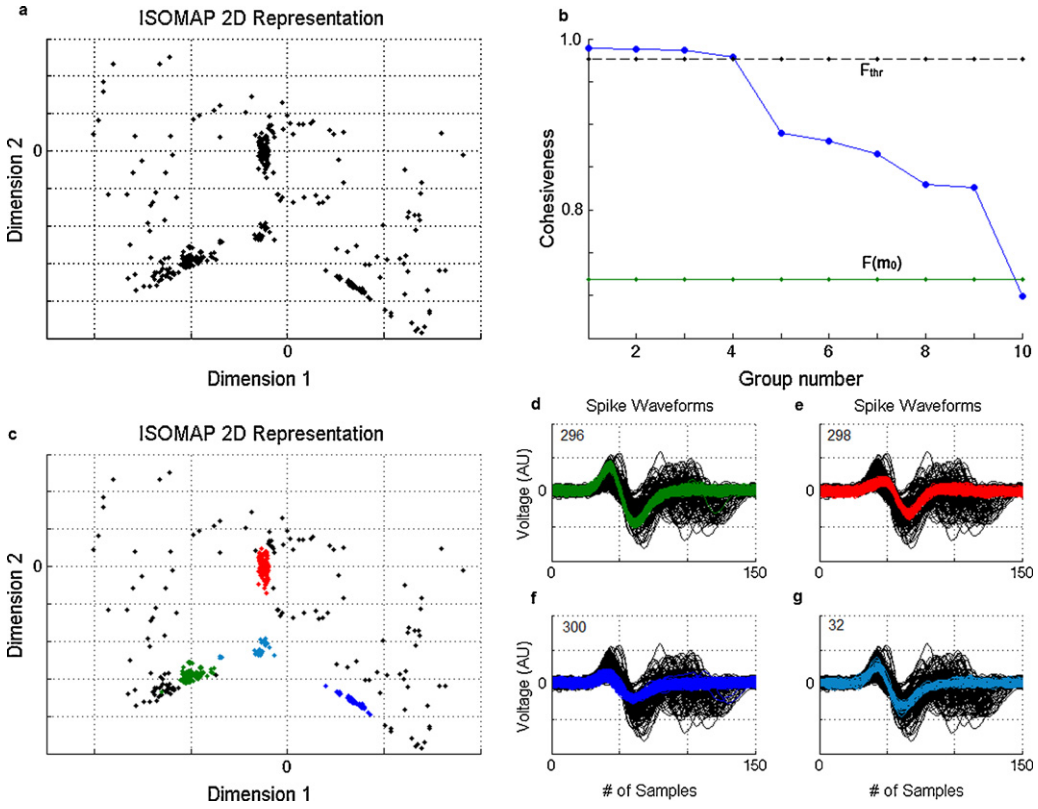

Fig. 3 – (a) 2D ISOMAP representation of a particular data set, augmented with 30 waveforms from a sparsely firing neuron (SNR = 4). (b) Group-cohesiveness values for the progressively formed groups (indicating the presence of four active neurons). (c) Classification visualized within 2D ISOMAP space. Colors indicate classes. (d–g) Classification results presented in the original data domain and using the corresponding colors. (For interpretation of the references to color in this figure legend, the reader is referred to the web version of the article.)

The validation in this case should be focused on the detection of the sparsely-firing neuron. Thus, we evaluated our algorithm, in a comparative fashion, against Waveclus regarding this particular task. For this reason, we defined the (relative) error-rate for this neuron as:

$$\text{Error-rate} = \frac{\Sigma_{\text{sparsely-firing neuron}}(Fp + Fn)}{\#\text{ of waveforms of the sparsely-firing neuron}} \times 100\% \quad (7)$$

The main parameter of the super-paramagnetic clustering algorithm employed in Waveclus, is the *Temperature* τ [7]. According to the manual, at low temperatures all spikes will be assigned to a single cluster, while at the high temperature limit every spike will form a cluster. The optimal temperature for clustering lies in between this two extremes (the 'super-paramagnetic regime'). The freely available Waveclus software incorporates an automated procedure for identifying the optimal temperature τ_o (an iterative scheme that includes the execution of Waveclus with different τ-values and the selection of the particular output clustering that maximizes the objective-function).

During our experimentations, the execution of Waveclus in its fully automated mode failed to identify the correct number of neurons in most of the cases (this trend has been reported in [17] as well). In these cases, the estimated (relative) error as defined in (7) exceeded 100%. To cope with this inconsistency and for the sake of fairness, we set manually the parameter τ so as the Waveclus to result in a cluster for the sparsely-firing neuron ($\tau = 0.02$ was a typical value for the temperature parameter, much lower than the optimal τ_o). Furthermore, to improve the performance, the 'force membership' option of the Waveclus software was exploited (points that were located far from any cluster or in between two clusters were assigned to the closest one).

The averaged (over different realizations) error-rates are drawn in Fig. 4 as a function of SNR. Even with manual tuning,

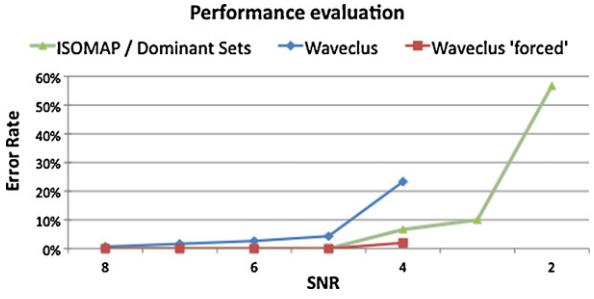

Fig. 4 – Relative (average) error rates for the task of identifying the sparsely-firing neuron activity.

Waveclus failed to identify the presence of the sparsely-firing neuron when SNR dropped below 4. On the other hand, our algorithm failed when SNR dropped to 1.5 and resulted in excessive error rate only at the lowest step (SNR = 2).

In high and medium SNR cases, Waveclus operating in 'force membership' mode (denoted as 'forced' in Fig. 4) performed equally well with our algorithm or better (in one SNR case). However, the performance of our method in detecting the other neurons remained intact, while the corresponding error rate (Eq. (6)) for Waveclus was raised by an average of 3% when 'force membership' mode was employed.

4. Conclusions

Experimental evidence [20–23] confirms earlier proposals [34,35] that the highest organization level of the brain is relatively "silent". Cortical neurons discharge rather sparsely. Thus, in a coding scheme referred to as sparse coding, the activity of a small number of select neurons can be very informative about the stimulus [36]. A characteristic example of information shaping stems from the study of the visual system. Out of the 10^{10} bits/s available to the retina only 6×10^6 leave the retina and only 10^4 make it to the visual cortical layers while estimates of the bandwidth of conscious awareness are in the range of 100 bits/s or less [37,38]. The functional importance of sparse activity is further highlighted by the fact that electrical stimulation of even a single sensory cortical neuron can lead to behavioral responses [39]. In the light of these findings, there is an increasing need for spike sorting algorithms to be optimized for the detection and correct classification of rarely spiking neurons.

The present work introduces a graph-theoretical framework for spike sorting. The core algorithm iteratively pursuits a dominant set in the graph (the most dominant in each iteration) and then removes it, until all data have been clustered. The efficiency of the proposed clustering method has been combined with the robustness of ISOMAP representation. The new hybrid scheme has been extensively evaluated. The results indicate high robustness to noise and a measured performance that goes beyond the contemporary standards.

Due to the subtractive nature of the algorithm, the number of active neurons needs not to be known in advance. Moreover, the introduced implementation guarantees the ability to mine small-sized groups of waveforms corresponding to sparsely firing neurons. It is also important to notice that some important issues like the treatment of overlaps and bursting activity were not discussed here and will be the focus of our future research efforts.

REFERENCES

[1] I. Cohen, R. Miles, Contribution of intrinsic and synaptic activities to the generation of neuronal discharges in vitro hippocampus, J. Physiol. 524 (2) (2000) 485–502.

[2] C. Gold, D.A. Henze, C. Koch, G. Buzsáki, On the origin of the extracellular action potential waveform: a modeling study, J. Neurophysiol. 95 (5) (2006) 3113–3128.

[3] E.M. Glaser, W.B. Marks, On-line separation of interleaved neuronal pulse sequences, Data Acquis. Process Biol. Med. 5 (1968) 137–156.

[4] M. Abeles, M.H. Goldstein, Multispike train analysis, Proc. IEEE 65 (1997) 762–773.

[5] J.C. Letelier, P.P. Weber, Spike sorting based on discrete wavelet transform coefficients, J. Neurosci. Methods 101 (2) (2000) 93–106.

[6] E. Hulata, R. Segev, E. Ben-Jacob, A method for spike sorting and detection based on wavelet packets and Shannon's mutual information, J. Neurosci. Methods 117 (1) (2002) 1–12.

[7] R. Quian Quiroga, Z. Nadasdy, Y. Ben-Shaul, Unsupervised spike detection and sorting with wavelets and superparamagnetic clustering, Neural Comput. 16 (8) (2004) 1661–1687.

[8] D.A. Adamos, E.K. Kosmidis, G. Theophilidis, Performance evaluation of PCA-based spike sorting algorithms, Comput. Methods Programs Biomed. 91 (3) (2008) 232–244.

[9] M. Lewicki, A review of methods for spike sorting: the detection and classification of neural action potentials, Netw. Comput. Neural Syst. 9 (1998) R53–R78.

[10] K.D. Harris, D.A. Henze, J. Csicsvari, H. Hirase, G. Buzsaki, G accuracy of tetrode spike separation as determined by simultaneous intracellular and extracellular measurements, J. Neurophysiol. 84 (1) (2000) 401–414.

[11] C. Pouzat, O. Mazor, G. Laurent, Using noise signature to optimize spike-sorting and to assess neuronal classification quality, J. Neurosci. Methods 122 (1) (2002) 43–57.

[12] M.S. Fee, P.P. Mitra, D. Kleinfeld, Variability of extracellular spike waveforms of cortical neurons, J. Neurophysiol. 76 (6) (1996) 3823–3833.

[13] A. Bar-Hillel, A. Spiro, E. Stark, Spike sorting: Bayesian clustering of non-stationary data, J. Neurosci. Methods 157 (2) (2006) 303–316.

[14] S. Grün, M. Diesmann, A. Aertsen, Unitary events in multiple single-neuron spiking activity: II. Nonstationary data, Neural Comput. 14 (1) (2002) 81–119.

[15] S. Takahashi, Y. Anzai, Y. Sakurai, Automatic sorting for multi-neuronal activity recorded with tetrodes in the presence of overlapping spikes, J. Neurophysiol. 89 (4) (2003) 2245–2258.

[16] M.S. Fee, P.P. Mitra, D. Kleinfeld, Automatic sorting of multiple unit neuronal signals in the presence of anisotropic and non-Gaussian variability, J. Neurosci. Methods 69 (2) (1996) 175–188.

[17] J.A. Herbst, S. Gammeter, D. Ferrero, R.H. Hahnloser, Spike sorting with hidden Markov models, J. Neurosci. Methods 174 (1) (2008) 126–134.

[18] F. Franke, M. Natora, C. Boucsein, M.H. Munk, K. Obermayer, An online spike detection and spike classification algorithm capable of instantaneous resolution of overlapping spikes, J. Comput. Neurosci. 29 (1–2) (2010) 127–148.

[19] R.H. Hahnloser, A.A. Kozhevnikov, M.S. Fee, An ultra-sparse code underlies the generation of neural sequences in a songbird, Nature 419 (6902) (2002) 65–70.

[20] B.A. Olshausen, D.J. Field, Sparse coding of sensory inputs, Curr. Opin. Neurobiol. 14 (4) (2004) 481–487.

[21] C. Pedreira, F. Mormann, A. Kraskov, M. Cerf, I. Fried, C. Koch, R. Quian Quiroga, Responses of human medial temporal lobe neurons are modulated by stimulus repetition, J. Neurophysiol. 103 (1) (2010) 97–107.

[22] R. Quian Quiroga, L. Reddy, G. Kreiman, C. Koch, I. Fried, Invariant visual representation by single neurons in the human brain, Nature 435 (7045) (2005) 1102–1107.

[23] R. Quian Quiroga, L. Reddy, C. Koch, I. Fried, Decoding visual inputs from multiple neurons in the human temporal lobe, J. Neurophysiol. 98 (4) (2007) 1997–2007.

[24] M. Pavan, M. Pelillo, Dominant sets and pairwise clustering, IEEE Trans. Pattern Anal. Mach. Intell. 29 (1) (2007) 167–172.
[25] J.B. Tenenbaum, V. de Silva, J.C. Langford, A global geometric framework for nonlinear dimensionality reduction, Science 290 (5500) (2000) 2319–2323.
[26] D.A. Adamos, N.A. Laskaris, E.K. Kosmidis, G. Theophilidis, Spike sorting based on dominant-sets clustering, in: R. Magjarevic, P.D. Bamidis, N. Pallikarakis (Eds.), XII Mediterranean Conference on Medical and Biological Engineering and Computing 2010, IFMBE Proc., 29, Springer, Berlin Heidelberg, 2010, pp. 5–8.
[27] N.A. Laskaris, A.A. Ioannides, Semantic geodesic maps: a unifying geometrical approach for studying the structure and dynamics of single trial evoked responses, Clin. Neurophysiol. 113 (8) (2002) 1209–1226.
[28] D.A. Adamos, N.A. Laskaris, E.K. Kosmidis, G. Theophilidis, NASS: an empirical approach to spike sorting with overlap resolution based on a hybrid noise-assisted methodology, J. Neurosci. Methods 190 (1) (2010) 129–142.
[29] C. Vargas-Irwin, J.P. Donoghue, Automated spike sorting using density grid contour clustering and subtractive waveform decomposition, J. Neurosci. Methods 164 (1) (2007) 1–18.
[30] G.L. Wang, Y. Zhou, A.H. Chen, P.M. Zhang, P.J. Liang, A robust method for spike sorting with automatic overlap decomposition, IEEE Trans. Biomed. Eng. 53 (6) (2006) 1195–1198.
[31] D.L. Donoho, De-noising by soft-thresholding, IEEE Trans. Inf. Theory 41 (3) (1995) 613–627.
[32] K.S. Guillory, R.A. Normann, A 100-channel system for real time detection and storage of extracellular spike waveforms, J. Neurosci. Methods 91 (1–2) (1999) 21–29.
[33] G. Zafeiridou, G. Theophilidis, The action of the insecticide imidacloprid on the respiratory rhythm of an insect: the beetle Tenebrio molitor, Neurosci. Lett. 365 (3) (2004) 205–209.
[34] R. Dykes, Y. Lamour, Neurons without demonstrable receptive fields outnumber neurons having receptive fields in samples from the somatosensory cortex of anesthetized or paralyzed cats and rats, Brain Res. 440 (1) (1988) 133–143.
[35] H.B. Barlow, Single units and sensation: a neuron doctrine for perceptual psychology? Perception 1 (4) (1972) 371–394.
[36] J. Wolfe, A.R. Houweling, M. Brecht, Sparse and powerful cortical spikes, Curr. Opin. Neurobiol. 20 (3) (2010) 306–312.
[37] C.H. Anderson, D.C. van Essen, B.A. Olshausen, Directed visual attention and the dynamic control of information flow, in: L. Itti, G. Rees, J. Tsotsos (Eds.), Neurobiology of attention, Elsevier, San Diego California, 2005, pp. 11–17.
[38] T. Norretranders, The User Illusion, Viking, New York, 1998.
[39] A.R. Houweling, M. Brecht, Behavioural report of single neuron stimulation in somatosensory cortex, Nature 451 (7174) (2008) 65–68.